Robotica (2013) volume 31, pp. 1229–1238. © Cambridge University Press 2013
doi:10.1017/S0263574713000325

Regressor-free prescribed performance robot tracking

Y. Karayiannidis†* and Z. Doulgeri‡

†*Computer Vision and Active Perception Lab., Centre for Autonomous Systems, School of Computer Science and Communication, Royal Institute of Technology (KTH), SE-100 44 Stockholm, Sweden*
‡*Department of Electrical and Computer Engineering, Aristotle University of Thessaloniki, Thessaloniki 54124, Greece*

(Accepted April 9, 2013. First published online: May 29, 2013)

SUMMARY
Fast and robust tracking against unknown disturbances is required in many modern complex robotic structures and applications, for which knowledge of the full exact nonlinear system is unreasonable to assume. This paper proposes a regressor-free nonlinear controller of low complexity which ensures prescribed performance position error tracking subject to unknown endogenous and exogenous bounded dynamics assuming that joint position and velocity measurements are available. It is theoretically shown and demonstrated by a simulation study that the proposed controller can guarantee tracking of the desired joint position trajectory with *a priori* determined accuracy, overshoot and speed of response. Preliminary experimental results to a simplified system are promising for validating the controller to more complex structures.

KEYWORDS: Tracking; Prescribed performance; Regressor-free controller; Robotic arm.

Nomenclature

$\boldsymbol{q}$, $\boldsymbol{q}_d(t) \in \Re^n$	Joint position and desired joint position trajectory.
e, $\boldsymbol{\varepsilon}$, $\boldsymbol{\varepsilon}_s \in \Re^n$	Joint position error, transformed error and saturated transformed error.
$\rho_i(t)$	Prescribed performance function for the ith joint.
ρ_{0i}, $\rho_{\infty i}$, l_i $M_i \in \Re^+$	Prescribed performance function parameters and overshot index for the ith joint.
$T_i(\bullet)$, J_{Ti}, J'_{Ti}	Transformation function and its first and second normalized partial derivative for the ith joint.
k_p, $\beta \in \Re$	Positive control constants.
$\boldsymbol{D} \in \Re^{n\times n}$	Positive definite diagonal control gain matrix.
$\dot{\boldsymbol{q}}_r \in \Re^n$	Reference velocity control signal.
$\boldsymbol{s} \in \Re^n$	Combined error.
Ω_{Vm}, Ω_{VM}, $\mathcal{E}$, Ω_ε	State regions.
$V(\boldsymbol{s}, \boldsymbol{\varepsilon}, t)$, $\sigma(\|\boldsymbol{\varepsilon}\|)$	Scalar functions.
$\bar{A}$, $\bar{B}$, $\bar{R}$, $\bar{\mu}$, $\bar{\sigma} \in \Re$	Constant bounds of $A(t)$, $B(t)$, $R(t)$, $\mu(t)$, $\sigma(t)$.
A_∞, B_∞, R_∞, μ_∞, $\sigma_\infty \in \Re$	Constants denoting the $\limsup_{t\to+\infty}$ of $A(t)$, $B(t)$, $R(t)$, $\mu(t)$, $\sigma(t)$.
λ_H, $c_0 \in \Re$	Constants related to the robot inertia matrix.
$\bar{F} \in \Re$	Constant bound of gravitational force $\boldsymbol{g}(\boldsymbol{q})$ and external disturbance $\boldsymbol{F}(t)$.
$\xi \in \Re$	Strictly positive free parameter.

* Corresponding author. E-mail: yiankar@kth.se

1. Introduction

It is known that in order to make robots perform many tasks, for example laser-cutting, plasma welding or high-speed operations in the presence of obstacles, trajectory tracking capabilities are necessary. Most of the different approaches for the robust control of robot manipulators for tracking are based on the knowledge of robot's nonlinear model or the exact knowledge of the regressor.[1–3] Alternatively, approximation structures, e.g. neural networks, have been employed in robot tracking controllers.[4] However, modern robotic systems like exoskeletons or light weight robots operating in a wide range of conditions and interacting with unknown environments do not allow us to account on the knowledge of a precise dynamical model or regressor. On the other hand, approximation structures demand to *a priori* guarantee that the developed controller confines the system state within the compact set in which the approximation capabilities hold, a task that requires most of the times a painful trial and error procedure for specifying the control gains, the initial parameter estimates and the basis functions. There exist, however, simple control schemes which do not rely on feedback linearisation or the use of a regressor or approximation structure and achieve robust stability in trajectory tracking by injecting high gain into the system;[5–7] they usually involve complex gain conditions making the determination of favourable control gains a difficult procedure. As pointed out in the latest survey on robust control of robot manipulators,[3] despite the considerable number of publications, nearly always the question of how a given set of performance specifications can be attained is left unanswered and a comparison to standard PD, proportional-integral-derivative (PID) controllers is seldom given. However, in some applications, such as the rehabilitation robotics, it is important to control the time

https://doi.org/10.1017/S0263574713000325 Published online by Cambridge University Press

attributes of the tracking errors.[8] Although few works address transient performance in robot manipulators,[8, 9] the achieved performance is not pre-specified with the exception of the funnel controller[10] in which prescribed performance (PP) is however related to a combined joint position and velocity error.

Lately, a control method that allows us to impose certain specifications on the performance of the system output in affine in the control nonlinear systems was introduced and is called the prescribed performance control method.[11] Key idea in prescribed performance is the introduction of an error transformation that modulates its components with respect to the corresponding required performance bounds imposed via performance functions of time and overshoot constants. This idea has been exploited in the model-based (regressor-based) robot tracking controllers[12, 13] and robot position regulators.[14–16] In our recently published paper,[17] it is shown that the prescribed performance of the joint position tracking error response is possible via a PD controller enhanced by a proportional term of the transformed error that does not however allow to set zero overshoot specification which is of high importance in robotic applications where robots and humans share the same workspace. This severe drawback is amended in the controller proposed in this work; it is a regressor-free controller for achieving PP position error tracking which allows zero overshoot specifications as opposed to the aforementioned controller.[17] Prescribed performance is guaranteed despite the existence of unknown endogenous and exogenous bounded dynamics, assuming that joint position and velocity measurements are available.

The rest of the paper is organized as follows: In Section 2, the robot dynamic model, its properties and preliminaries on PP control methodology are given. Section 3 is devoted to the controller design and theoretical proof, with details given in appendices, for joint position trajectory tracking with *a priori* determined accuracy, arbitrary overshoot and speed of response. In Section 4 the proposed scheme is validated and compared with a simple PID controller via simulations with a 3 degrees of freedom (DoF) manipulator and experiments with a simplified system, and lastly, conclusions are drawn in Section 5.

2. Problem Description

Let us consider an n-DoF robotic manipulator with revolute joints. Our main objective is to design a regressor-free dynamic controller that achieves the tracking of the desired joint position trajectory $\boldsymbol{q}_d(t) \in \Re^n$ with guaranteed PP specifications – including zero overshoot – for the joint position error $\boldsymbol{e}(t) = \boldsymbol{q}(t) - \boldsymbol{q}_d(t) \in \Re^n$. Dropping the time argument for presentation compactness from the above-defined variables and their corresponding derivatives, we can write the Euler–Lagrange equations describing the dynamic model of the robot as follows:

$$\boldsymbol{H}(\boldsymbol{q})\ddot{\boldsymbol{q}} + \boldsymbol{C}(\boldsymbol{q}, \dot{\boldsymbol{q}})\dot{\boldsymbol{q}} + \boldsymbol{C}_v\dot{\boldsymbol{q}} + \boldsymbol{g}(\boldsymbol{q}) + \boldsymbol{F}(t) = \boldsymbol{u}(t), \quad (1)$$

where $\boldsymbol{H}(\boldsymbol{q}) \in \Re^{n\times n}$ is the positive definite inertia matrix, i.e. $\boldsymbol{H}(\boldsymbol{q}) = \boldsymbol{H}^T(\boldsymbol{q}) > 0, \quad \forall \boldsymbol{q} \in \Re^n, \quad \boldsymbol{C}(\boldsymbol{q}, \dot{\boldsymbol{q}})\dot{\boldsymbol{q}} \in \Re^n$ denotes the centripetal and Coriolis force vector, $\boldsymbol{g}(\boldsymbol{q}) \in \Re^n$ is the gravity force vector, $\boldsymbol{C}_v \in \Re^{n\times n}$ denotes the positive diagonal matrix of viscous joint friction coefficients, $\boldsymbol{F}(t) \in \Re^n$ denotes any bounded model dynamic error or disturbance force and $\boldsymbol{u}(t)$ is the joint input vector. Note that joint Coulomb friction and the LuGre dynamical friction model can be accommodated in model (1).

2.1. Properties of the robot dynamic model

Some of the basic properties for revolute joint manipulators exploited in this work are given below:

$$\lambda_h \boldsymbol{I}_n \le \boldsymbol{H}(\boldsymbol{q}) \le \lambda_H \boldsymbol{I}_n, \quad (2)$$

$$\boldsymbol{C}(\boldsymbol{q}, \boldsymbol{a})\boldsymbol{b} = \boldsymbol{C}(\boldsymbol{q}, \boldsymbol{b})\boldsymbol{a} \quad \forall\, \boldsymbol{a}, \boldsymbol{b} \in \Re^n, \quad (3)$$

$$\boldsymbol{C}(\boldsymbol{q}, \boldsymbol{a} + \boldsymbol{b}) = \boldsymbol{C}(\boldsymbol{q}, \boldsymbol{a}) + \boldsymbol{C}(\boldsymbol{q}, \boldsymbol{b}) \quad \forall\, \boldsymbol{a}, \boldsymbol{b} \in \Re^n, \quad (4)$$

$$\|\boldsymbol{C}(\boldsymbol{q}, \boldsymbol{a})\boldsymbol{b}\| \le c_0\|\boldsymbol{a}\|\|\boldsymbol{b}\| \quad \forall\, \boldsymbol{a}, \boldsymbol{b} \in \Re^n, \quad (5)$$

$$\boldsymbol{y}^T\left(\dot{\boldsymbol{H}}(\boldsymbol{q}) - 2\boldsymbol{C}(\boldsymbol{q}, \dot{\boldsymbol{q}})\right)\boldsymbol{y} = 0 \quad \forall\, \boldsymbol{y} \in \Re^n, \quad (6)$$

$$\dot{\boldsymbol{H}}(\boldsymbol{q}) = \boldsymbol{C}^T(\boldsymbol{q}, \dot{\boldsymbol{q}}) + \boldsymbol{C}(\boldsymbol{q}, \dot{\boldsymbol{q}}), \quad (7)$$

$$\boldsymbol{S}(\boldsymbol{q}, \dot{\boldsymbol{q}}) = \boldsymbol{C}^T(\boldsymbol{q}, \dot{\boldsymbol{q}}) - \boldsymbol{C}(\boldsymbol{q}, \dot{\boldsymbol{q}}), \quad (8)$$

where $\lambda_h \triangleq \min_{\boldsymbol{q}\in\Re^n}[\lambda_m(\boldsymbol{H}(\boldsymbol{q}))]$, $\lambda_H \triangleq \max_{\boldsymbol{q}\in\Re^n}[\lambda_M(\boldsymbol{H}(\boldsymbol{q}))]$, c_0 are positive constants, $\lambda_m(\cdot)$ and $\lambda_M(\cdot)$ denote the minimum and the maximum eigenvalue of a matrix, respectively, and $\|\cdot\|$ denotes the Euclidean norm of a vector. A comprehensive presentation of the properties of the robot dynamic model can be found in textbooks.[18]

2.2. Prescribed performance

This section summarizes preliminary knowledge on PP control.[19] Prescribed performance is achieved if each element $e_i, i = 1, \ldots, n$ of the tracking error $\boldsymbol{e}$ evolves within predefined time-dependent bounds that can be mathematically expressed as follows:

$$-M_i\rho(t) < e_i < \rho_i(t) \qquad \text{in case of} \quad e_{0i} \ge 0, \quad (9)$$

$$-\rho_i(t) < e_i < M_i\rho_i(t) \qquad \text{in case of} \quad e_{0i} \le 0 \quad (10)$$

for $i = 1, \ldots, n$, where $0 \le M_i \le 1$ is the overshoot index, $i = 1, \ldots, n$, $e_{0i} \triangleq e_i(0)$, $i = 1, \ldots, n$ and $\rho_i(t)$, $i = 1, \ldots, n$ are smooth, bounded, strictly positive and decreasing functions of time satisfying $\limsup_{t\to+\infty}\rho_i(t) > 0$, $i = 1, \ldots, n$ called performance functions. Without loss of generality they can be decaying functions of time with a $\lim_{t\to+\infty}\rho_i(t) > 0$, $i = 1, \ldots, n$ being set to a value smaller than the required accuracy, thus achieving practical convergence of e_i to zero. In this work, the exponential function is used, i.e.

$$\rho_i(t) = (\rho_{0i} - \rho_{\infty i})\exp(-l_i t) + \rho_{\infty i}, \quad (11)$$

where ρ_{0i}, l_i and $\rho_{\infty i}$ are strictly positive constants appropriately chosen by the designer denoting $\rho_i(0)$, the minimum required speed of convergence, and the maximum allowable size of the tracking error at the steady state.

https://doi.org/10.1017/S0263574713000325 Published online by Cambridge University Press

The maximum overshoot of e_i is prescribed less than $M_i\rho_i(0)$ and it may even take a zero value by setting $M_i = 0$. In order to satisfy bound (9) or (10) at $t = 0$, ρ_{0i} is selected such that $\rho_i(0) > |e_{0i}|$ for $|e_{0i}| > 0$, where $|\cdot|$ denotes the absolute value of a scalar, or M_i is selected strictly positive when $e_{0i} = 0$. As it is implied by bound (9) or (10), only one set of performance bounds is employed for each $e_i(t)$, the one associated with the sign of e_{0i}; either bound (9) or (10) can be used in case of $e_{0i} = 0$.

To satisfy both tracking and prescribed performance for the joint position error, an error transformation is employed. More specifically, the components $\varepsilon_i(t)$ of the transformed error $\boldsymbol{\varepsilon}(t) \in \Re^n$ are defined as follows:

$$\varepsilon_i(t) = T_i\left(\frac{e_i}{\rho_i(t)}\right), \tag{12}$$

where $T_i(\cdot)$, $i = 1, \ldots, n$ are smooth, strictly increasing functions defining onto mappings:

$$T_i : (-M_i, 1) \to (-\infty, \infty) \quad \text{in case of} \quad e_{0i} \geq 0, \tag{13}$$

$$T_i : (-1, M_i) \to (-\infty, \infty) \quad \text{in case of} \quad e_{0i} \leq 0 \tag{14}$$

for $i = 1, \ldots, n$.

The following natural logarithm function which satisfies the aforementioned properties can be used in (12) so that zero overshoot specifications can be imposed[19]:

$$T_i\left[\frac{e_i}{\rho_i(t)}\right] = \ln\left(\frac{M_i + \frac{e_i}{\rho_i(t)}}{1 - \frac{e_i}{\rho_i(t)}}\right) \quad \text{in case of } e_{0i} \geq 0, \tag{15}$$

$$T_i\left[\frac{e_i}{\rho_i(t)}\right] = \ln\left(\frac{1 + \frac{e_i}{\rho_i(t)}}{M_i - \frac{e_i}{\rho_i(t)}}\right) \quad \text{in case of } e_{0i} \leq 0. \tag{16}$$

Note that the trajectory tracking controller of our previous work[17] requires a transformation function with $T_i(0) = 0$ which does not allow a zero overshoot specification. Zero overshoot is an important property in robotics and can be guaranteed by the controller proposed in this work. As implied by (15) and (16) the choice of mapping depends only on the sign of e_{0i}. A graphical illustration of this function is provided in Fig. 1.

The satisfaction of PP bounds concerning the tracking error $\boldsymbol{e}$ is directly related to the boundedness of the transformed error $\boldsymbol{\varepsilon}(t)$. In fact, given $|\varepsilon_i(t)| \leq \bar{\varepsilon}$, for some positive constant $\bar{\varepsilon}$, the actual tracking error is restricted $\forall t \geq 0$ as follows:

$$-M_i\rho(t) < -\underline{K}_i\rho_i(t) \leq e_i \leq \bar{K}_i\rho_i(t) < \rho_i(t) \text{ for } e_{0i} \geq 0,$$

$$-\rho_i(t) < -\bar{K}_i\rho_i(t) \leq e_i \leq \underline{K}_i\rho_i(t) < M_i\rho_i(t) \text{ for } e_{0i} \leq 0,$$

where $\bar{K}_i$ and $\underline{K}_i$ are positive constants satisfying $\underline{K}_i < M_i$, $\bar{K}_i < 1$ and $\underline{K}_i \leq \bar{K}_i$. Figure 1 is illustrative of this restriction for the case of an error component. Hence, in the ball $B_{\bar{\varepsilon}} \triangleq \{\boldsymbol{\varepsilon}(t) \in \Re^n : \|\boldsymbol{\varepsilon}(t)\| \leq \bar{\varepsilon}\}$, wherein $|\varepsilon_i(t)| \leq \bar{\varepsilon}$, the following inequality holds:

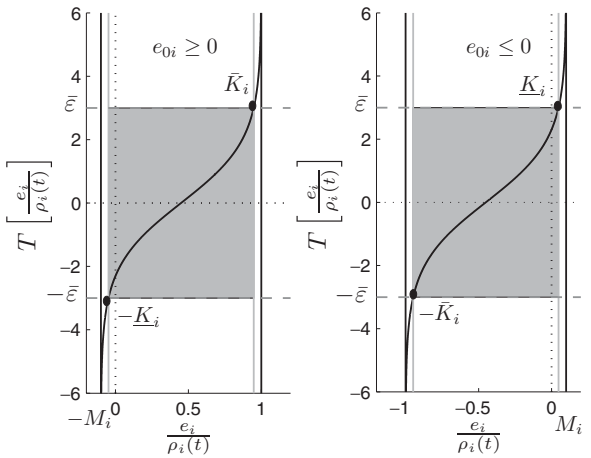


Fig. 1. Error transformation with natural logarithm.

$$\left|\frac{e_i}{\rho_i(t)}\right| \leq \bar{K}_i < 1. \tag{17}$$

Clearly, by (i) ensuring that the initial value of $\varepsilon_i(t)$ is bounded, which is realized by setting $\rho_{0i} > |e_{0i}| > 0$ and $M_i \neq 0$ in case of $e_{0i} = 0$, and (ii) designing a controller to guarantee that $\varepsilon_i(t)$ remains bounded $\forall t > 0$ is sufficient to impose PP bounds on the tracking error e_i that will evolve strictly within the performance region and will not even asymptotically approach its boundary. Note that the magnitude of the bound of the transformed error $\bar{\varepsilon}$ is not related to the evolution of the tracking error that is solely defined by bounds (9) and (10).

3. Controller Design

We propose the following regressor-free controller:

$$\boldsymbol{u}(t) = -k_p\boldsymbol{J}_T(t)\boldsymbol{\varepsilon}(t) - \boldsymbol{D}\boldsymbol{s}(t), \tag{18}$$

where k_p is a positive control gain, $\boldsymbol{D}$ is a positive definite diagonal gain matrix, the components of $\boldsymbol{\varepsilon}(t)$ are defined by (12) and $\boldsymbol{J}_T(t) \triangleq \text{diag}\,[J_{T1}(t), \ldots, J_{Tn}(t)]$ with positive and away from zero entries is defined by:

$$J_{Ti}(t) \triangleq \frac{\partial T_i}{\partial(e_i/\rho_i(t))}\frac{1}{\rho_i(t)} > 0, \tag{19}$$

and $\boldsymbol{s}(t) \triangleq \dot{\boldsymbol{q}} - \dot{\boldsymbol{q}}_r(t)$ denotes the error between the joint velocity and the reference velocity, $\dot{\boldsymbol{q}}_r(t)$, that is designed as follows:

$$\dot{\boldsymbol{q}}_r(t) = \dot{\boldsymbol{q}}_d - \boldsymbol{\alpha}(t)\boldsymbol{e} - \beta\boldsymbol{J}_T^{-1}(t)\boldsymbol{\varepsilon}_s(t), \tag{20}$$

where β is a positive control constant, $\boldsymbol{\alpha}(t)$ is a diagonal matrix with positive entries defined by:

$$\alpha_i(t) = -\frac{\dot{\rho}_i(t)}{\rho_i(t)} > 0 \text{ with } \lim_{t\to+\infty}\alpha_i(t) = 0, \tag{21}$$

https://doi.org/10.1017/S0263574713000325 Published online by Cambridge University Press

and $\boldsymbol{\varepsilon}_s(t)$ is an n-dimensional vector with components $\varepsilon_{si}(t) = \text{sat}(\varepsilon_i(t))$ and sat$(\cdot)$ denotes any odd, bounded and increasing function with a positive definite integral with respect to $\varepsilon_i(t)$. Examples of sat$(\cdot)$ functions are the hyperbolic tangent function, i.e. tanh$(\cdot)$ as well as the partial derivative of quasi-natural potential functions.[20] Without loss of generality we consider $|\varepsilon_{si}| \leq 1$ and $|\frac{\partial \varepsilon_{si}}{\partial \varepsilon_i}| \leq 1$, which imply:

$$\|\boldsymbol{\varepsilon}_s\| \leq \sqrt{n} \qquad \|\frac{\partial \boldsymbol{\varepsilon}_s}{\partial \boldsymbol{\varepsilon}}\| \leq \sqrt{n}. \tag{22}$$

Furthermore, we define the scalar function $\sigma(\|\boldsymbol{\varepsilon}(t)\|) \triangleq \boldsymbol{\varepsilon}^T(t)\boldsymbol{\varepsilon}_s(t)$ that is invertible and satisfies the inequality $\sigma(\|\boldsymbol{\varepsilon}(t)\|) \leq c\|\boldsymbol{\varepsilon}(t)\|^2$ for some $c > 0$.

Remark 1. The proposed controller provides damping to the system through the feedback of the error between the current velocity and an appropriately designed reference velocity. Despite the complicated structure of this controller, the use of $\dot{\boldsymbol{q}}_r$ instead of $\dot{\boldsymbol{q}}_d$ utilized in our previous work[17] enables (i) a zero overshoot specification, which is important in robotic applications by allowing the use of a transformation with $T_i(0) \neq 0$, and (ii) the tuning of an extra control parameter β in order to achieve smoother control input response as well as admissible control input values.

Note that using (20), $\boldsymbol{s}(t)$ can be written as a combined error:

$$\boldsymbol{s}(t) = \dot{\boldsymbol{e}} + \boldsymbol{\alpha}(t)\boldsymbol{e} + \beta \boldsymbol{J}_T^{-1}(t)\boldsymbol{\varepsilon}_s(t). \tag{23}$$

Differentiating (12) with respect to time, we obtain:

$$\dot{\boldsymbol{\varepsilon}}(t) = \boldsymbol{J}_T(t)[\dot{\boldsymbol{e}} + \boldsymbol{\alpha}(t)\boldsymbol{e}]. \tag{24}$$

Using (24) in (23) we can express $\boldsymbol{s}(t)$ with respect to $\boldsymbol{\varepsilon}(t)$ and its derivative as follows:

$$\boldsymbol{s}(t) = \boldsymbol{J}_T^{-1}(t)\left[\dot{\boldsymbol{\varepsilon}}(t) + \beta \boldsymbol{\varepsilon}_s(t)\right]. \tag{25}$$

In the following, the argument of time is dropped from $\dot{\boldsymbol{q}}_r(t)$, $\boldsymbol{s}(t)$, $\boldsymbol{\varepsilon}(t)$, $\boldsymbol{\varepsilon}_s(t)$ and $\boldsymbol{J}_T(t)$ for compactness of presentation. Substituting the input control law (18) in the robot dynamic model (1), adding and subtracting $\boldsymbol{H}(\boldsymbol{q})\ddot{\boldsymbol{q}}_r + \boldsymbol{C}(\boldsymbol{q}, \dot{\boldsymbol{q}})\dot{\boldsymbol{q}}_r + \boldsymbol{C}_v\dot{\boldsymbol{q}}_r + \boldsymbol{C}(\boldsymbol{q}, \dot{\boldsymbol{q}}_r)\dot{\boldsymbol{q}}_r$ and taking (4) into consideration, we can write the closed loop system as follows:

$$\begin{aligned}\boldsymbol{H}(\boldsymbol{q})\dot{\boldsymbol{s}} + \boldsymbol{C}(\boldsymbol{q}, \dot{\boldsymbol{q}})\boldsymbol{s} + k_p \boldsymbol{J}_T\boldsymbol{\varepsilon} + \boldsymbol{D}\boldsymbol{s} \\ + \boldsymbol{h}(\boldsymbol{q}, \dot{\boldsymbol{q}}_r, \ddot{\boldsymbol{q}}_r, \boldsymbol{s}, t) = 0,\end{aligned} \tag{26}$$

where

$$\begin{aligned}\boldsymbol{h}(\boldsymbol{q}, \dot{\boldsymbol{q}}_r, \ddot{\boldsymbol{q}}_r, \boldsymbol{s}, t) =& \boldsymbol{H}(\boldsymbol{q})\ddot{\boldsymbol{q}}_r + [\boldsymbol{C}(\boldsymbol{q}, \boldsymbol{s}) + \boldsymbol{C}(\boldsymbol{q}, \dot{\boldsymbol{q}}_r)]\dot{\boldsymbol{q}}_r \\ &+ \boldsymbol{C}_v\dot{\boldsymbol{q}}_r + \boldsymbol{g}(\boldsymbol{q}) + \boldsymbol{F}(t).\end{aligned} \tag{27}$$

Note that the use of the reference velocity in the control input enables the formulation of the system as first-order nonlinear differential equations with respect to the states $\boldsymbol{s}$, $\boldsymbol{\varepsilon} \in \Re^n$. As a result, we can intuitively use an energy function (49) that consists of a pseudo-kinetic energy of the manipulator based on the velocity error as well as the potential energy due to the transformed error control action in order to prove the main theorem of this work. Consequently, the stability analysis is significantly simplified.

We consider the following state space domain for the system (26):

$$\Omega_\varepsilon = \left\{\boldsymbol{s},\ \boldsymbol{\varepsilon} \in \Re^n :\ \boldsymbol{\varepsilon} \in B_{\bar{\varepsilon}}\right\}. \tag{28}$$

Note that $\boldsymbol{q}$, $\dot{\boldsymbol{q}}$, $\dot{\boldsymbol{q}}_r$, $\ddot{\boldsymbol{q}}_r$ and $\boldsymbol{J}_T$ appear in a closed loop system (26), can be expressed with respect to the system state $\boldsymbol{s}$, $\boldsymbol{\varepsilon}$ and the time variable t. The analysis below consists of three propositions (the corresponding proofs can be found in Appendix B) leading to the main theorem of this work.

Proposition 1. Given $\boldsymbol{q}_d \in \mathcal{C}^2$ and $\dot{\boldsymbol{q}}_d \in \mathcal{L}_\infty$, the reference velocity $\dot{\boldsymbol{q}}_r$ is bounded $\forall \boldsymbol{s},\ \boldsymbol{\varepsilon} \in \Omega_\varepsilon$:

$$\|\dot{\boldsymbol{q}}_r\| \leq\ R(t) \leq \bar{R}, \quad \forall \boldsymbol{s},\ \boldsymbol{\varepsilon} \in \Omega_\varepsilon,\ \forall t \geq 0, \tag{29}$$

where

$$\begin{aligned}R(t) =& \|\dot{\boldsymbol{q}}_d\| \\ &+ \sqrt{n}\left[\max_i(|\dot{\rho}_i(t)|) + \beta \max_i\left(\rho_i(t)\frac{M_i + 1}{4}\right)\right]\end{aligned} \tag{30}$$

$$\begin{aligned}\text{with } \bar{R} =& \max_t(\|\dot{\boldsymbol{q}}_d\|) + \sqrt{n}\left[\max_i(l(\rho_{0i} - \rho_{\infty i}))\right. \\ &\left. + \beta \max_i\left(\rho_{0i}\frac{M_i + 1}{4}\right)\right],\end{aligned} \tag{31}$$

$$\begin{aligned}R_\infty \triangleq& \limsup_{t\to\infty} R(t) = \limsup_{t\to\infty} \|\dot{\boldsymbol{q}}_d\| \\ &+ \sqrt{n}\beta \max_i\left(\rho_{\infty i}\frac{M_i + 1}{4}\right).\end{aligned} \tag{32}$$

Proposition 2. Given $\boldsymbol{q}_d \in \mathcal{C}^2$ and $\ddot{\boldsymbol{q}}_d \in \mathcal{L}_\infty$, the derivative of reference velocity denoted by $\ddot{\boldsymbol{q}}_r$ satisfies the following inequality $\forall \boldsymbol{s},\ \boldsymbol{\varepsilon} \in \Omega_\varepsilon$:

$$\begin{aligned}&\|\ddot{\boldsymbol{q}}_r\| \leq A(t) + B(t)\|\boldsymbol{s}\| \leq \bar{A} + \bar{B}\|\boldsymbol{s}\|, \\ &\forall \boldsymbol{s}, \boldsymbol{\varepsilon} \in \Omega_\varepsilon, \forall t \geq 0,\end{aligned} \tag{33}$$

https://doi.org/10.1017/S0263574713000325 Published online by Cambridge University Press

where

$$A(t) = \|\ddot{\boldsymbol{q}}_d\| + \beta\sqrt{n}\max_i\left(\rho_i(t)\frac{M_i+1}{4}\right)\left[\max_i(|\alpha_i(t)|) + B(t)\right] + \sqrt{n}\max_i(|\ddot{\rho}_i(t)|) \le \bar{A}, \tag{34}$$

$$B(t) = \max_i(|\alpha_i(t)|) + \max_i\left(\frac{4\beta}{M_i+1}\right) \le \bar{B}, \tag{35}$$

$$\bar{A} = \max_t(\|\ddot{\boldsymbol{q}}_d\|) + \beta\sqrt{n}\max_i\left[\rho_{0i}\left(\beta + \frac{M_i+1}{2}l_i\right)\right] \tag{36}$$

$$+ \sqrt{n}\max_i\left(l_i^2(\rho_{0i} - \rho_{\infty i})\right), \tag{37}$$

$$\bar{B} = \max_i(l_i) + \max_i\left(\frac{4\beta}{M_i+1}\right) \tag{38}$$

and

$$A_\infty \triangleq \limsup_{t\to\infty} A(t) = \limsup_{t\to\infty}\|\ddot{\boldsymbol{q}}_d\| + \beta^2\sqrt{n}\max_i(\rho_{\infty i}), \tag{39}$$

$$B_\infty \triangleq \limsup_{t\to\infty} B(t) = \max_i\left(\frac{4\beta}{M_i+1}\right). \tag{40}$$

Proposition 3. Given that the gravitational and disturbance forces are bounded as follows:

$$\|\boldsymbol{g}(\boldsymbol{q}) + \boldsymbol{F}(t)\| \le \bar{F}, \tag{41}$$

with $\bar{F}$ being a positive constant, the following inequality holds $\forall \boldsymbol{s},\ \boldsymbol{\varepsilon} \in \Omega_\varepsilon$

$$\boldsymbol{s}^T\boldsymbol{h}(\boldsymbol{q}, \dot{\boldsymbol{q}}_r, \ddot{\boldsymbol{q}}_r, \boldsymbol{s}, t) \ge -(\mu(t) + d(t)\|\boldsymbol{s}\|^2) \ge -(\bar{\mu} + \bar{d}\|\boldsymbol{s}\|^2),\ \forall \boldsymbol{s},\ \boldsymbol{\varepsilon} \in \Omega_\varepsilon,\ \forall t \ge 0, \tag{42}$$

where $\mu(t)$ and $d(t)$ are positive and bounded $\forall t \ge 0$:

$$\mu(t) = \frac{\xi^2}{2}\left[\bar{F}^2 + (\lambda_H A(t))^2 + c_0^2R^4(t) + c_v^2R^2(t)\right] \le \bar{\mu}, \tag{43}$$

$$d(t) = \lambda_H B(t) + c_0R(t) + \frac{3}{2\xi^2} \le \bar{d}, \tag{44}$$

with ξ being some strictly positive constant and

$$\bar{\mu} = \frac{\xi^2}{2}\left[\bar{F}^2 + (\lambda_H\bar{A})^2 + c_0^2\bar{R}^4 + c_v^2\bar{R}^2\right], \tag{45}$$

$$\bar{d} = \lambda_H\bar{B} + c_0\bar{R} + \frac{3}{2\xi^2}. \tag{46}$$

Propositions 1, 2 and 3 are valid under the assumption that $\boldsymbol{s},\ \boldsymbol{\varepsilon} \in \Omega_\varepsilon$. In the following theorem, we establish that the proposed control law does not force $\boldsymbol{s}, \boldsymbol{\varepsilon}$ solutions to escape Ω_ε at any point of time t, where Propositions 1–3 hold. We shall prove this argument by showing that there exists an invariant set contained in Ω_ε and hence starting within this set the system state cannot escape from it.

Theorem. *Consider the state domain Ω_ε and the closed loop system (26) with a choice of gain matrix $\boldsymbol{D}$ satisfying the following condition:*

$$\lambda_m(\boldsymbol{D}) > \bar{d} \text{ where } \bar{d} = \lambda_H\bar{B} + c_0\bar{R} + \frac{3}{2\xi^2}. \tag{47}$$

Then, (a) the region $\mathcal{E}$:

$$\mathcal{E} = \left\{\boldsymbol{s}, \boldsymbol{\varepsilon} \in \Re^n : \boldsymbol{s}^T(\boldsymbol{D} - d(t)\boldsymbol{I}_n)\boldsymbol{s} + \beta k_p\sigma(\|\boldsymbol{\varepsilon}\|) < \mu(t)\right\}, \tag{48}$$

is bounded and is a subset of Ω_ε for some finite $\bar{\varepsilon}$, (b) the positive definite, radially unbounded and decrescent scalar function

$$V(\boldsymbol{s}, \boldsymbol{\varepsilon}, t) = \frac{1}{2}\boldsymbol{s}^TH(\boldsymbol{q})\boldsymbol{s} + \frac{1}{2}k_p\|\boldsymbol{\varepsilon}\|^2 \tag{49}$$

has a negative derivative along the system trajectories in the region $\Omega_\varepsilon - \mathcal{E}$, (c) starting within a bounded region defined by a Lyapunov surface, the state of the closed loop system is confined within this bounded region and (d) the joint position tracking error $\boldsymbol{e}$ respects the prescribed performance bounds imposed by bounds (9) and (10).

Proof. (a) Clearly, (47) and $\mu(t) \le \bar{\mu}\ \forall \boldsymbol{s},\ \boldsymbol{\varepsilon} \in \Omega_\varepsilon$ imply that $\mathcal{E}$ is bounded. Using the function $V(\boldsymbol{s}, \boldsymbol{\varepsilon}, t)$ in (49), we can define the region Ω_{Vm}:

$$\Omega_{Vm} = \{\boldsymbol{s},\ \boldsymbol{\varepsilon} \in \Re^n :\ V(\boldsymbol{s}, \boldsymbol{\varepsilon}, t) \le \kappa\} \tag{50}$$

for some positive constant κ such that $\mathcal{E} \subset \Omega_{Vm}$. We can also define the region Ω_{VM}:

$$\Omega_{VM} = \left\{\boldsymbol{s},\ \boldsymbol{\varepsilon} \in \Re^n :\ V(\boldsymbol{s}, \boldsymbol{\varepsilon}, t) \le \frac{1}{2}k_p\bar{\varepsilon}^2\right\} \tag{51}$$

for some positive constant $\bar{\varepsilon}$ such that $\Omega_{Vm} \subset \Omega_{VM}$; by construction, $\Omega_{VM} \subset \Omega_\varepsilon$. The aforementioned regions are illustrated in Fig. 2.

(b) Differentiating $V(\boldsymbol{s}, \boldsymbol{\varepsilon}, t)$, substituting $\dot{\boldsymbol{s}}$ from (26) and $\dot{\boldsymbol{\varepsilon}}$ from (25) and subsequently using (6) yields the following:

$$\frac{dV(\boldsymbol{s}, \boldsymbol{\varepsilon}, t)}{dt} = -k_p\beta\boldsymbol{\varepsilon}_s^T\boldsymbol{\varepsilon} - \boldsymbol{s}^T(\boldsymbol{D} + \boldsymbol{C}_v)\boldsymbol{s} - \boldsymbol{s}^Th(\boldsymbol{q}, \dot{\boldsymbol{q}}_r, \ddot{\boldsymbol{q}}_r, \boldsymbol{s}, t). \tag{52}$$

Using (42) of Proposition 3 that is valid in the domain Ω_ε and subsequently in the closed region Ω_{VM}, (52) yields:

$$\frac{dV(\boldsymbol{s}, \boldsymbol{\varepsilon}, t)}{dt} \le -k_p\beta\boldsymbol{\varepsilon}_s^T\boldsymbol{\varepsilon} - \boldsymbol{s}^T(\boldsymbol{D} - d(t)\boldsymbol{I}_n)\boldsymbol{s} + \mu(t), \tag{53}$$

which is negative definite with respect to $\boldsymbol{\varepsilon}$ and $\boldsymbol{s}$ outside the region $\mathcal{E}$. Hence, the derivative of $V(\boldsymbol{s}, \boldsymbol{\varepsilon}, t)$ is negative in the region $\Omega_\varepsilon - \mathcal{E}$ and consequently in the region $\Omega_{VM} - \Omega_{Vm}$.

https://doi.org/10.1017/S0263574713000325 Published online by Cambridge University Press

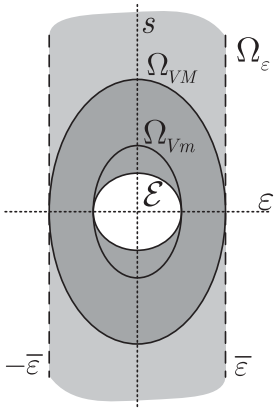


Fig. 2. Illustration of regions.

(c) Note that we have selected M_i, ρ_{0i}, $i = 1, \ldots, n$ to satisfy bound (9) or (10) at $t = 0$ and that the initial joint velocity and its corresponding desired value are assumed bounded. Hence, the initial system solution $\boldsymbol{\varepsilon}(0)$, $\boldsymbol{s}(0)$ is well defined. In order to prove the boundedness of the system state $\forall t > 0$ we distinguish two cases (i) $\boldsymbol{s}(0)$, $\boldsymbol{\varepsilon}(0) \in \Omega_{Vm}$ and (ii) $\boldsymbol{s}(0)$, $\boldsymbol{\varepsilon}(0) \in \Omega_{VM} - \Omega_{Vm}$. In case (i), $\boldsymbol{s}$ and $\boldsymbol{\varepsilon}$ remain in Ω_{Vm}, $\forall t > 0$, since $dV(\boldsymbol{s}, \boldsymbol{\varepsilon}, t)/dt \leq 0$ on the boundary of Ω_{Vm}; hence, $\boldsymbol{s}(t)$, $\boldsymbol{\varepsilon}(t) \in \Omega_{Vm}$, $\forall\, t > 0$, which in turn implies $\boldsymbol{s}$, $\boldsymbol{\varepsilon} \in \mathcal{L}_\infty$. In case (ii), $V(\boldsymbol{s}(0), \boldsymbol{\varepsilon}(0), 0) \leq \frac{1}{2} k_p \bar{\varepsilon}^2$ and $V(\boldsymbol{s}(t), \boldsymbol{\varepsilon}(t), t) \leq V(\boldsymbol{s}(0), \boldsymbol{\varepsilon}(0), 0)$, $\forall t > 0$ since $dV(\boldsymbol{s}, \boldsymbol{\varepsilon}, t)/dt \leq 0$ in $\Omega_{VM} - \Omega_{Vm}$ and consequently $\boldsymbol{s}$, $\boldsymbol{\varepsilon}$ cannot escape from Ω_{VM} and thus $\boldsymbol{s}$, $\boldsymbol{\varepsilon} \in \mathcal{L}_\infty$. In this case, the system state will finally converge to the region Ω_{Vm}, which is the UUB region. The boundedness of $\boldsymbol{s}$, $\boldsymbol{\varepsilon}$ implies that $\boldsymbol{J}_T$ and $\boldsymbol{u}$ are bounded. By setting $\bar{\varepsilon} \geq \sqrt{\frac{2 \max[V(\boldsymbol{s}(0), \boldsymbol{\varepsilon}(0), 0), \kappa]}{k_p}}$ we guarantee that the theorem is valid for any finite $\boldsymbol{\varepsilon}(0)$, $\boldsymbol{s}(0)$.

(d) For any $\boldsymbol{\varepsilon}(0)$ satisfying bound (9) or (10) at $t = 0$, $\boldsymbol{\varepsilon}(0)$ is bounded and given (c) $\boldsymbol{\varepsilon}$ remains bounded. The boundedness of $\boldsymbol{\varepsilon}$ implies that the joint position tracking error $\boldsymbol{e}$ evolves within the PP bound (9) or (10). □

Remark 2. In the theorem, following Theorem 4.18,[21] we have proved the UUB of the system state with respect to the set Ω_{Vm} in local sense ($\forall \boldsymbol{s}$, $\boldsymbol{\varepsilon} \in \Omega_\varepsilon$) by finding an invariant set Ω_{VM} containing the UUB region Ω_{Vm}. Note that $\bar{\varepsilon}$, which can be regarded as the magnitude of the invariant set, can always be chosen such that $\bar{\varepsilon} \geq \sqrt{\frac{2 \max[V(\boldsymbol{s}(0), \boldsymbol{\varepsilon}(0), \boldsymbol{q}(0)), \kappa]}{k_p}}$ implying a semi-global result, i.e. for any finite $\boldsymbol{\varepsilon}(0)$, $\boldsymbol{s}(0)$, the states $\boldsymbol{\varepsilon}$, $\boldsymbol{s}$ remain bounded and after a time period they converge to the UUB region Ω_{Vm}.

Remark 3. Note that the gain lower bound (47) involves the prescribed performance parameters in $\bar{B}$ and $\bar{R}$ that are known and the constants λ_H and c_0 that are related to the robot dynamic model defined in (2) and (5), respectively, and consist the only system information required to be known or estimated. In case of high uncertainty, overestimates of λ_H and c_0 can be utilized that cannot affect the prescribed performance for the position tracking error but may lead to higher values of the control input.

Remark 4. Note that the joint position tracking error $\boldsymbol{e}$ respects the performance bounds irrespective of the magnitude of the UUB region (50). On the other hand, reducing the UUB region benefits the joint velocity error which is involved in $\boldsymbol{s}$. In particular, using (61) of Appendix A, (21) and $\lim_{t \to +\infty} \rho(t) = \rho_\infty$, (23) implies:

$$\limsup_{t \to +\infty} \|\dot{\boldsymbol{e}}\| \leq \limsup_{t \to +\infty} \|\boldsymbol{s}\| + \beta \frac{\rho_\infty (M_i + 1)}{4} \limsup_{t \to +\infty} \|\boldsymbol{\varepsilon}_s\|$$

The magnitudes of $\limsup_{t \to +\infty} \|\boldsymbol{s}\|$ and $\limsup_{t \to +\infty} \|\boldsymbol{\varepsilon}_s\|$ are proportional to the magnitude of Ω_{Vm} and consequently proportional to the magnitude of $\mathcal{E}$. The region $\mathcal{E}$ shrinks to a region with size related inversely proportionally to the gain values $\boldsymbol{D}$ and k_p and proportionally to the values of μ_∞, d_∞ that are given below:

$$\mu_\infty \triangleq \limsup_{t \to +\infty} \mu(t) = \frac{\xi^2}{2} \left[\bar{F}^2 + (\lambda_H A_\infty)^2 + c_0^2 R_\infty^4 + c_v^2 R_\infty^2 \right], \quad (54)$$

$$d_\infty \triangleq \limsup_{t \to +\infty} d(t) = \lambda_H B_\infty + c_0 R_\infty + \frac{3}{2\xi^2}. \quad (55)$$

Constant μ_∞ (54) can be made arbitrarily small by considering small values of the free design variable ξ which however adversely affect d_∞ (55) and $\bar{d}$ (46). The value of ξ that minimizes $\mathcal{E}$, i.e. $\xi^\star = \arg\min_\xi (\mathcal{E}_v)$ is given by

$$\xi^\star = \sqrt{\frac{3}{\lambda_m(\boldsymbol{D}) - \lambda_H B_\infty - c_0 R_\infty}}.$$

Remark 5. Theoretically, the proposed solution considers the unconstrained input case. However, the control input is proved bounded and its range depends on the choice of appropriate values for control parameters. Although there is no constructive procedure to find the optimal gain values for a minimum energy cost, one can use optimization tools for determining the gain values that minimize the control effort, e.g. genetic algorithms and simulation of the system. Note that the control gain selection does not affect the speed of convergence, the maximum allowed overshoot and steady state error which are a priori set and guaranteed.

4. Simulation and Experimental Results

4.1. Simulation results

We consider a spatial 3-DoF robotic arm shown in Fig. 3 with masses $m_1 = m_2 = 5$ kg, $m_3 = 2.5$ kg, lengths $l_1 = l_2 = 1$ m, $l_3 = 0.5$ m, inertias $I_{z1} = I_{y2} = I_{z2} = 0.4208$ kg m^2, $I_{y3} = I_{z3} = 0.0542$ kg m^2. The robot is required to track the following desired joint trajectory $[30, 40, 50]^T (1 - \cos 2\pi t)$ (deg) starting from an initial position 5 deg for each joint respectively. This implies the existence of an initial position error at $\boldsymbol{e}(0) = 8.73\ 10^{-2} [\ 1\ \ 1\ \ 1\ ]^T$ (rad). The performance function is selected for each joint as follows: $\rho_i(t) =$

https://doi.org/10.1017/S0263574713000325 Published online by Cambridge University Press

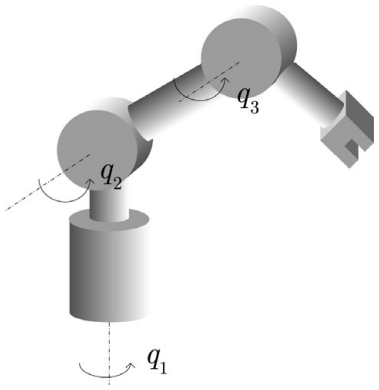


Fig. 3. A spatial 3-DoF robotic arm used for simulation.

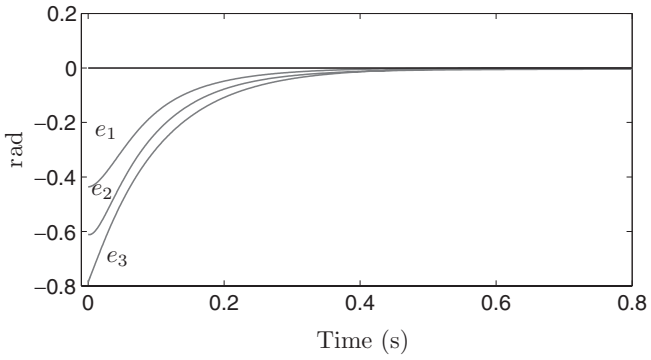


Fig. 4. Position error responses in a regulation case with a PID controller.

$(0.15 - 10^{-3})e^{-4t} + 10^{-3}$ implying a 1 s settling time and a maximum steady state error of 10^{-3} rad. The overshoot index is set to zero, $M_i = 0$. Control gain values are: $k_p = 1$, $\boldsymbol{D} = \text{diag}[300, 450, 300]$ and $\beta = 1$.

The following PID controller is also implemented using an internal velocity feedback[22]:

$$u_{\text{PID}i} = -k_{vi}\left[T_{vi}(\dot{e} + k_{pi}e) + \int_0^t (\dot{e} + k_{pi}e)d\tau\right]. \quad (56)$$

PID gain values were carefully tuned to achieve an overdamped response with speed comparable to the decaying rate of the performance function as shown by the error responses in Fig. 4 in a regulation scenario for set-points located in the middle of the peak-to-peak response of the desired trajectory, i.e. $[30, 40, 50]^T$ (deg). PID gain values are: $k_{v1} = 80$, $k_{v2} = 400$, $k_{v3} = 120$, $T_{v1} = 3.75$, $T_{v2} = 1$, $T_{v3} = 2.5$, $k_{p1} = k_{p2} = k_{p3} = 10$. The proposed controller was additionally subjected to a disturbance input given by $\boldsymbol{F}(t) = [60, 120, 18] \sin 2\pi t$ (Nm) introduced in the system at 1 s having a magnitude comparable to the required input torques (Fig. 8(b)).

Figures 5 and 6 show responses of the joint position tracking error and the velocity error norm, respectively, produced with the proposed regressor-free PP controller and the PID controller. When the robot is controlled with the proposed PP controller, position errors respect the performance bounds and the velocity norm remains robust even after the introduction of the disturbance input at 1 s.

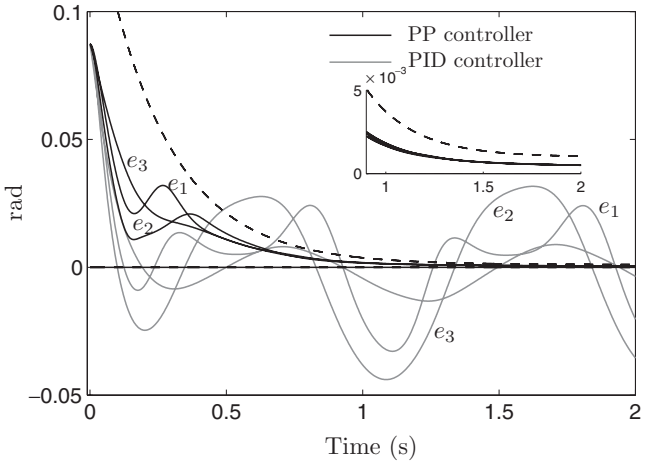


Fig. 5. Position error responses (solid lines) and performance bounds (dashed lines).

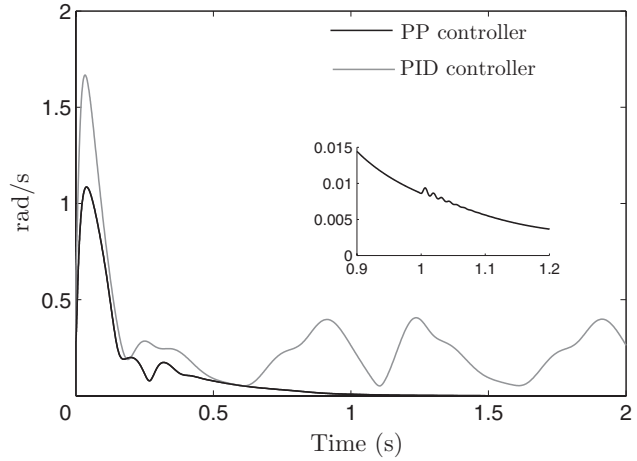


Fig. 6. Norm of velocity error.

Respective responses with the PID controller, even in the absence of the disturbance input, exhibit much higher errors reflecting the high gravitational force value changes during the robot motion. Very good performance and robustness achieved by the proposed controller does not demand an excessive control effort with respect to the PID as shown in Figs. 7 and 8 which depict input torques without consideration of gear reduction ratios that are usually present in joint actuators. Figure 8 shows PP control input torques under both presence and absence of the disturbance input which is also displayed. Note how the control input adjusts to the disturbance in order to satisfy the prescribed performance for the position tracking error.

4.2. Experimental results

A 1-DoF experimental setup is used to validate theoretical and simulation results. It consists of a DC motor (Faulhaber 2342024CR) equipped with an incremental encoder and a low rate reduction gear box (1:14) driven by Maxon Motor's analogue ADS Servoamplifier 50/5 in current mode which implements an internal current loop and a link of 15 cm length and 145 g total mass moving in the gravity field. Joint velocity is calculated through the use of a filter. Controllers are

https://doi.org/10.1017/S0263574713000325 Published online by Cambridge University Press

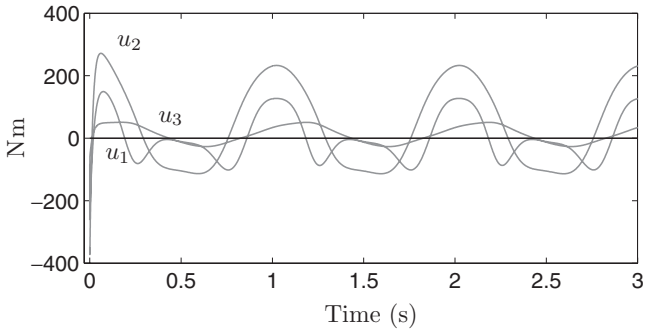


Fig. 7. Input torques with the PID controller in case of zero disturbances.

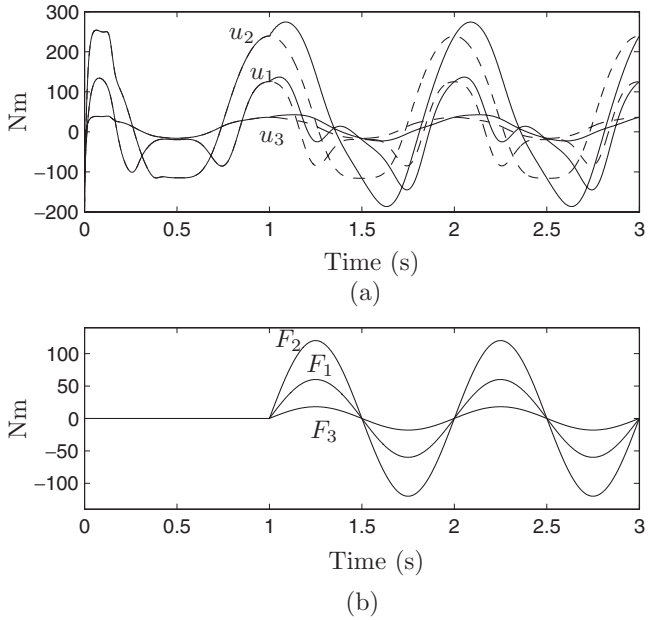


Fig. 8. (a) Input torques with the PP controller in case of input disturbances (solid line) and zero disturbances (dashed line), (b) input disturbances.

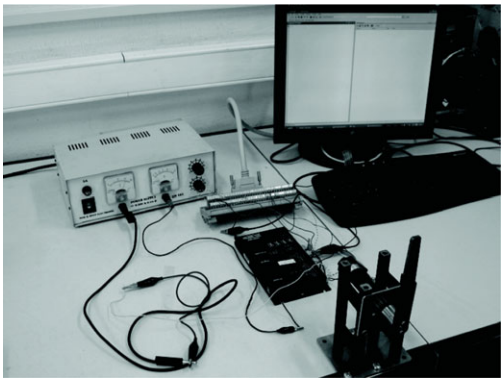


Fig. 9. (Colour online) Experimental setup.

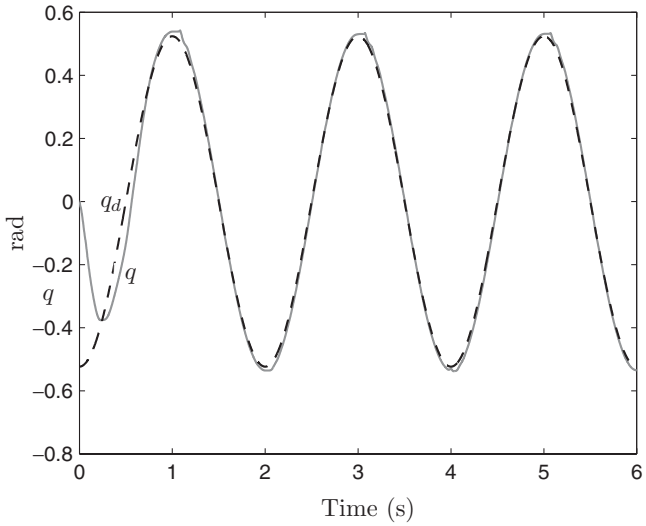


Fig. 10. Joint position and desired trajectories.

implemented in Simulink Matlab with 1-ms sampling time. The experimental setup is shown in Fig. 9. Our simplified experimental setup enables the preliminary validation of the proposed controller in operational conditions met in practical applications, including non-negligible nonlinearities due to low gear ratio, measurement noise, discretization and bounded input values.

The proposed regressor-free prescribed performance controller as well as the PID controller (56) is implemented for comparison purposes. The tracking of the desired trajectory of $-30\cos\pi t$ deg starting from the unstable equilibrium of the link which implies an initial error of $e(0) = \pi/6$ rad is required. The following performance function $\rho(t) = (\pi/6 - \pi/90)e^{-4t} + \pi/90$ is prescribed, implying a settling time of 1 s and a maximum allowed steady state error of 10^{-2} rad. Gain values, $D = 0.5$, $\beta = 8$ and $k_p = 0.008$, are used and the overshoot index is set to $M = 1$. PID gains are chosen so that closed loop poles correspond to an overdamped response with speed comparative to that of the prescribed performance for the unloaded motor; their values are: $k_p = 9.5$, $k_v = 1.5574$, $T_v = 0.314$.

Figure 10 shows the actual and desired joint trajectories and Fig. 11 shows the joint position error response, including the response of the system under the PID controller (solid grey line) for comparison purposes. Note that the nonlinear system disturbances are reflected to the error response in case of PID control in contrast to the error response in case of PP control which respects the predefined bounds. The input torque responses are shown in Fig. 12 for both prescribed performance and PID controllers. Note that the torque magnitudes of both control inputs are comparable and do not meet the motor saturation bounds, which are ±5 V.

5. Conclusions

This work proposes a low complexity regressor-free robot joint tracking controller achieving the evolution of the position tracking error within the PP bounds which are designed to reflect *a priori* set values for the minimum speed of convergence, the maximum allowed steady state error and the overshoot index that can be set to zero. It is proved that the proposed controller achieves prescribed performance for the position tracking error and UUB for the

https://doi.org/10.1017/S0263574713000325 Published online by Cambridge University Press

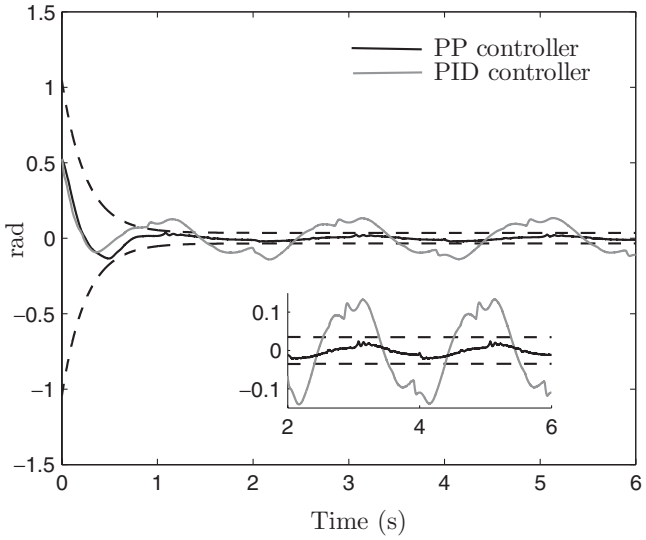


Fig. 11. Error response.

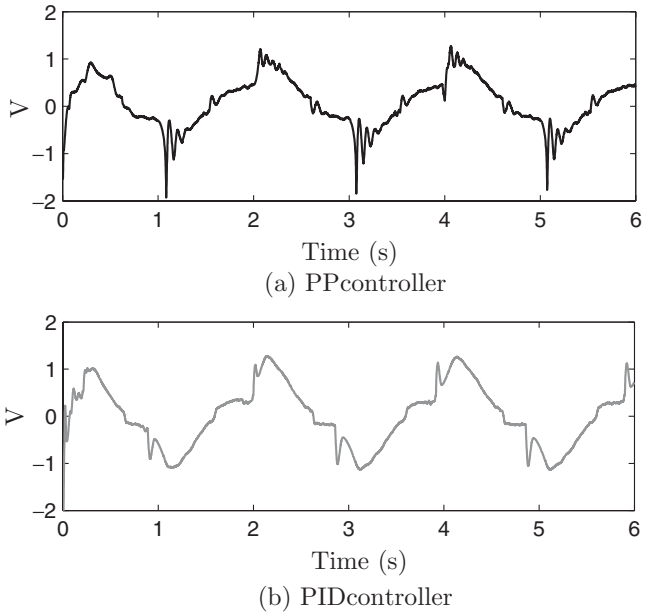


Fig. 12. Input torque responses.

velocity error given that the damping gains dominate a lower bound involving characteristic constants of the robot inertia matrix. Control gain selection is significantly simplified and merely confined to achieve admissible input torques. Simulation responses with the PP controller for a 3-DoF spatial arm confirm the theoretical findings even in case of significant input disturbances outperforming responses produced by a carefully tuned PID controller operating in the absence of the disturbance input without demanding excessive control effort. Preliminary experimental results show that the proposed controller achieves the control objective, outperforming a typical low-gain PID controller with comparable control effort. Despite the use of a simplified system, experimental results are promising for validating the controller to more complex structures.

Acknowledgment

Y. Karayiannidis is supported by the Swedish Foundation for Strategic Research.

References

1. M. W. Spong, S. Hutchinson and M. Vidyasagar, *Robot Modelling and Control* (John Wiley, Somerset, New Jersey, 2006).
2. J. Slotine and W. Li, *Applied Nonlinear Control* (Prentice Hall, Upper Saddle River, New Jersey, 1993).
3. H. Sage, M. D. Mathelin and E. Ostertag, "Robust control of robot manipulators: A survey," *Int. J. Control* **72**, 1498–1522 (1999).
4. F. Lewis, S. Jagannathan and A. Yeşildirek, *Neural Netwrok Control of Robot Manipulators and Nonlinear Systems* (Taylor & Francis, Boca Raton, Florida, 1999).
5. S. Kawamura, F. Miyazaki and S. Arimoto, "Is a Local Linear PD Feedback Control Law Effective for Trajectory Tracking of Robot Motion?," **In**: *Proceedings of the IEEE International Conference in Robotics and Automation*, Philadelphia (1988) pp. 1335–1340.
6. J. Wen and S. Murphy, "PID Control for Robot Manipulators," *CIRSSE Document #54* (Rensselaer Polytechinc Institute, Troy, New York, May 1990).
7. Z. Qu and J. Dorsey, "Robust PID control of robots," *Int. J. Robot. Autom.* **6**(4), 228–235 (1991).
8. L. Lugo-Villeda, A. Frisoli, V. Parra-Vega and M. Bergamasco, "Regressor-Free Force/Position Control of Fixed-Base Exoskeletons for Rehabilitation Tasks," **In**: *IEEE/RSJ International Conference on Intelligent Robots and Systems, 2009 (IROS 2009)*, St. Louis (Oct. 2009) pp. 1639 –1645.
9. B. Yao and M. Tomizuka, "Adaptive robust motion and force tracking control of robot manipulators in contact with stiff surfaces," *ASME J. Dyn. Syst. Meas. Control*, **120**, 232–240 (1998).
10. C. M. Hackl, C. Endisch and D. Schröder, "Contributions to non-identifier based adaptive control in mechatronics," *Robot. Auton. Syst.* **57**(10), 996–1005 (2009).
11. C. Bechlioulis and G. Rovithakis, "Prescribed performance adaptive control for multi-input multi-output affine in the control nonlinear systems," *IEEE Trans. Autom. Control* **55**(5), 1220–1226 (2010).
12. C. Bechlioulis, Z. Doulgeri and G. Rovithakis, "Robot Force/Position Tracking with Guaranteed Prescribed Performance," **In**: *Proceedings of the IEEE International Conference in Robotics and Automation*, Kobe (2009), pp. 3688–3693.
13. Z. Doulgeri, Y. Karayiannidis and O. Zoidi, "Prescribed Performance Control for Robot Joint Trajectory Tracking Under Parametric and Model Uncertainties," **In**: *Proceedings of the IEEE 17th Mediterranean Conference on Control and Automation*, Thessaloniki (2009) pp. 1313–1318.
14. Z. Doulgeri and O. Zoidi, "Prescribed Performance Regulation for Robot Manipulators," **In**: *Proceedings of the 9th International IFAC Symposium on Robot Control (SYROCO '09)*, Gifu (2009) pp. 721–726.
15. Z. Doulgeri and Y. Karayiannidis, "PID Type Robot Joint Position Regulation with Prescribed Performance Guaranties," **In**: *Proceedings of the IEEE International Conference in Robotics and Automation*, Anchorage (2010) pp. 4137–4142.
16. Z. Doulgeri and L. Droukas, "Robot Task Space PID Type Regulation with Prescribed Performance Guaranties," **In**: *2010 IEEE/RSJ International Conference on Intelligent Robots and Systems (IROS)*, Taipei (2010) pp. 1644–1649.
17. Y. Karayiannidis and Z. Doulgeri, "Model-free robot joint position regulation and tracking with prescribed performance guarantees," *Robot. Auton. Syst.* **60**(2), 214–226 (2012).
18. R. Kelly, V. Santibáñez and A. Loría, *Control of Robot Manipulators in Joint Space* (Springer, New York, 2005).

https://doi.org/10.1017/S0263574713000325 Published online by Cambridge University Press

19. C. Bechlioulis and G. Rovithakis, "Robust adaptive control of feedback linearizable mimo nonlinear systems with prescribed performance," *IEEE Trans. Autom. Control* **53**(9), 2090–2099 (2008).
20. S. Arimoto, *Control Theory of Non-linear Mechanical Systems, A Passivity-Based and Circuit-Theoretic Approach* (Oxford University Press, Oxford, UK, 1996).
21. H. Khalil, *Nonlinear Systems*, 3rd ed. (Prentice Hall, Upper Saddle River, New Jersey, 2002).
22. B. Siciliano, L. Sciavicco, L. Villani and G. Oriolo, *Robotics: Modelling, Planning and Control* (Springer-Verlag, Berlin, Germany, 2009).

Appendix A. Performance and transformation functions properties

From (11) and (21) the following inequalities involving the performance function hold:

$$\rho_i(t) \leq \rho_{0i}, \tag{57}$$

$$|\dot{\rho}_i(t)| \leq l_i(\rho_{0i} - \rho_{\infty i}), \tag{58}$$

$$|\ddot{\rho}_i(t)| \leq l_i^2(\rho_{0i} - \rho_{\infty i}), \tag{59}$$

$$\alpha_i(t) < l_i. \tag{60}$$

From (15) and/or (16) and (19) the following inequalities involving the transformation function can be easily proved:

$$|J_{Ti}^{-1}| \leq \rho_i(t)\frac{M_i + 1}{4}, \tag{61}$$

$$\| \left(J_{Ti}^{-1}\right)^2 J'_{Ti}\| \leq \frac{3 - M_i}{1 + M_i}, \tag{62}$$

where $J'_{Ti} \triangleq \frac{1}{\rho_i^2}\frac{\partial^2}{\partial x^2}[T_i(x)]$ denotes the ith diagonal entry of the second normalized Jacobian $\boldsymbol{J}'_T$ of the transformation function.

Appendix B. Proofs of propositions

Proof of Proposition 1

Taking the norm of (20) and using the triangle inequality $\|\boldsymbol{a} + \boldsymbol{b}\| \leq \|\boldsymbol{a}\| + \|\boldsymbol{b}\|$ as well as (61) and (17) that is valid in Ω_ε, (22) and subsequently (57) and (58) we get (29).

Proof of Proposition 2

Differentiating (20), we obtain the reference acceleration $\ddot{\boldsymbol{q}}_r$; by expressing all terms with respect to $\boldsymbol{\varepsilon}$ and/or $\boldsymbol{\varepsilon}_s$ and $\dot{\boldsymbol{\varepsilon}}$ and substituting $\dot{\boldsymbol{\varepsilon}}$ with respect to $\boldsymbol{s}$ and $\boldsymbol{\varepsilon}_s$ from (25), $\ddot{\boldsymbol{q}}_r$ can be written as follows:

$$\ddot{\boldsymbol{q}}_r = \boldsymbol{A}_r(t) + \boldsymbol{B}_r(t)\boldsymbol{s}, \tag{63}$$

where

$$\begin{aligned}\boldsymbol{A}_r(t) &= \ddot{\boldsymbol{q}}_d + \operatorname{diag}\left\{\frac{\ddot{\rho}_i(t)}{\rho_i(t)}\right\}\boldsymbol{e} + \beta\boldsymbol{\alpha}(t)\boldsymbol{J}_T^{-1}\boldsymbol{\varepsilon}_s \\ &\quad - \beta\boldsymbol{B}_r(t)\boldsymbol{J}_T^{-1}\boldsymbol{\varepsilon}_s, \end{aligned}\tag{64}$$

$$\begin{aligned}\boldsymbol{B}_r(t) &= -\boldsymbol{\alpha}(t) + \beta(\boldsymbol{J}_T^{-1})^2\boldsymbol{J}'_T\operatorname{diag}\{\varepsilon_{si}\} \\ &\quad - \beta\operatorname{diag}\left\{\frac{\partial\varepsilon_{si}}{\partial\varepsilon_i}\right\}. \end{aligned}\tag{65}$$

Taking the norm of (64) and (65) and using the triangle inequality, (61), (17) that is valid in Ω_ε, (22) and subsequently (57), (59) and (60), we obtain (33).

Proof of Proposition 3

The proof uses the inequality $\boldsymbol{a}^T\boldsymbol{b} \leq \frac{1}{2\xi^2}\|\boldsymbol{a}\|^2 + \frac{\xi^2}{2}\|\boldsymbol{b}\|^2$, $\forall \boldsymbol{a}, \boldsymbol{b} \in \Re^n$, where $\boldsymbol{a}$ and $\boldsymbol{b}$ are n-dimensional vectors and ξ is a positive constant. Using (41) the product $-\boldsymbol{s}^T[\boldsymbol{g}(\boldsymbol{q}) + \boldsymbol{F}(t)]$ is upper-bounded as follows:

$$-\boldsymbol{s}^T[\boldsymbol{g}(\boldsymbol{q}) + \boldsymbol{F}(t)] \leq \|\boldsymbol{s}\|\,\bar{F} \leq \frac{1}{2\xi^2}\|\boldsymbol{s}\|^2 + \frac{\xi^2}{2}\bar{F}^2. \tag{66}$$

Using (33) and (2), $-\boldsymbol{s}^T\boldsymbol{H}(\boldsymbol{q})\ddot{\boldsymbol{q}}_r$ is upper-bounded as follows:

$$-\boldsymbol{s}^T\boldsymbol{H}(\boldsymbol{q})\ddot{\boldsymbol{q}}_r \leq \left[\lambda_H B(t) + \frac{1}{2\xi^2}\right]\|\boldsymbol{s}\|^2 + \frac{\xi^2}{2}[\lambda_H A(t)]^2, \tag{67}$$

where $A(t)$ and $B(t)$ are given by (34) and (35) respectively. Finally, using (5) the sum $-\boldsymbol{s}^T\boldsymbol{C}(\boldsymbol{q}, \boldsymbol{s})\,\dot{\boldsymbol{q}}_r - \boldsymbol{s}^T\boldsymbol{C}(\boldsymbol{q}, \dot{\boldsymbol{q}}_r)\dot{\boldsymbol{q}}_r - \boldsymbol{s}^T\boldsymbol{C}_v\dot{\boldsymbol{q}}_r$ is upper-bounded as follows:

$$\begin{aligned}&-\boldsymbol{s}^T\boldsymbol{C}(\boldsymbol{q}, \boldsymbol{s})\dot{\boldsymbol{q}}_r - \boldsymbol{s}^T\boldsymbol{C}(\boldsymbol{q}, \dot{\boldsymbol{q}}_r)\dot{\boldsymbol{q}}_r - \boldsymbol{s}^T\boldsymbol{C}_v\dot{\boldsymbol{q}}_r \\ &\quad \leq \left(c_0R(t) + \frac{1}{2\xi^2}\right)\|\boldsymbol{s}\|^2 + \frac{\xi^2}{2}\left(c_0^2R^4(t) + c_v^2R^2(t)\right), \end{aligned}\tag{68}$$

where $R(t)$ is given by (30) and c_v is maximum entry of $\boldsymbol{C}_v$. Combining (66)–(68) we obtain inequality (42).

https://doi.org/10.1017/S0263574713000325 Published online by Cambridge University Press